Optical-phase conjugation nonlinearity compensation in Flexi-Grid optical networks

C. Sánchez, M. Mccarthy, A. D. Ellis
Aston Institute of Photonic Technologies
School of Engineering and Applied Science
Birmingham B4 7ET, UK
c.sanchez-costa@aston.ac.uk

P. Wright, A. Lord
British Telecom
Adastral Park, Martlesham Heath
Ipswich, IP5 3RE, UK

Abstract: Optical-phase conjugation nonlinearity compensation (OPC-NLC) in optical networks is evaluated using a built-in tool including self-channel and crosstalk channel interference effects. Though significant improvements are observed, a further refined launch power policy is required to fully take advantage of OPC-NLC capability.

Key–Words: Nonlinearity compensation, optical networks.

1 Introduction

As the traffic demand continues to grow exponentially, telecom carriers need to upgrade optical networks in order to exploit more efficiently their inherent capacity. Techniques explored for this purpose range from more flexible transponders with adaptively modulation formats and launch powers, impairment-aware routing algorithms, to Flexi-grid wavelength-division multiplexing systems [1–3]. However, the ultimate limiting factor will be that imposed by fiber nonlinearities, which prevents higher values of signal power spectral densities increasing the optical-signal-to noise ratio (OSNR) [4, 5] indefinitely. Nonlinearity compensation (NLC) techniques aim to increase the launch power at which fiber nonlinearities start to significantly impair the received signal quality. Unlike digital-back propagation which suffers from bandwidth receiver limitations, optical-phase conjugation-based NLC is parallel in nature and compensates for both inter- and intra-channel nonlinear impairments [6].

Although mature for point-to-point transmission links, OPC remains as an unexplored area in the context of optical networks, where it is not possible to know a priori the path followed by any given signal, and neighboring channels may not have the same start and end points. In this paper we explore for the first time the benefits brought by OPC in optical networks. Specifically, we study the potential improvement as a function of the number of OPCs in an example optical network in terms of supported capacity. We include the effects of self-channel and crosstalk-channel nonlinear interference (SCI and XCI) impairments and optimise the capacity using: a variable modulation format selected according to the calculated nonlinear signal-to-noise ratio (SNR); a variable launch power value is adjusted according to the fraction of the fibre nonlinearity compensated for by the OPCs in each optical path, and a Flexi-grid wavelength allocation algorithm.

2 Optical network model

Simulations have been performed on the 20+2 node network shown in Fig. 1, where all nodes add/drop traffic except nodes 21 and 22 which provide connectivity to other sites. This network is an idealised simplification of the UK reference model. Each link in the network carry up to 5000 GHz of C-band spectrum, and no wavelength conversion or regeneration of signals occurred in the network. The network was sequentially loaded with bi-directional demands, with the source and destination nodes of each demand selected randomly among the 20 nodes with equal probability. The traffic demand was also randomly generated, taking one of the four possible values: 100, 200, 400 or 1000 Gbps. Table I shows the range of polarisation multiplexed modulation formats which could be selected to satisfy the traffic demand given the achieved SNR. Amplifiers had a noise figure equal to 5dB and a gain equal to the losses of each span; the fiber loss and nonlinear coefficient were equal to 0.2dB/km and 1.3×10^{-3}W/km; a channel initialisation margin M, explained in the next section, was equal to 2dB, and the required SNR, SNR_{req}, was set such the BER for each modulation format did not

Table 1: Traffic demands and modulation formats

Traffic demand	Possible Mod. Format
100 Gbps	QPSK, 8-, 16-QAM
200 Gbps	QPSK, 8-, 16-, 32-, 64-QAM
400 Gbps	QPSK, 8-, 16-, 32-, 64-, 128-, 256-QAM
1000 Gbps	QPSK, 8-, 16-, 32-, 64-, 128-, 256-, 512-, 1024-QAM

exceed 10^{-3} [10].

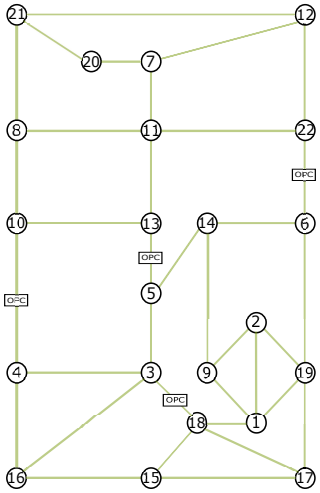

Figure 1: Reference core network topology. All the links of the network have four spans, except those linking nodes 1-2, 1-9,1-19, 2-9 and 2-19 which have two. The location of the four first placed OPCs is also depicted.

Signal routing and wavelength assignment were based on the minimum-hop path and first-fit spectrum algorithms [11]. We assumed that the signals transmitted were Nyquist-shaped signals, with a rectangular spectrum of width equal to the symbol rate. The power spectral density of the signals transmitted was linearly adjusted between the minimum and maximum values P_{min} and P_{max} as a function of the fraction of the spans whose nonlinear contributions are compensated for as:

$$P_{sig} = P_{min} + \frac{N_{SpansComp}}{N_{SpansPath}} \cdot \left(P_{max} - P_{min}\right) \quad (1)$$

We assumed the use of standard single-mode fiber periodically amplified by erbium doped fiber amplifiers. The span length was fixed throughout the network at 50 km. Spontaneous noise from the optical amplification process was modeled as additive Gaussian noise, with a dual-polarisation spectral density equal to [8] $P_N = (G-1) \cdot 2n_{sp} \cdot hv$ where G is the amplifier gain, n_{sp} is the spontaneous inversion factor, h is the Planck's constant, and v is the optical frequency. Fiber nonlinearity effects were modeled following [9] with the accumulation of SCI and XCI nonlinear impairments taking into account the existence of any ideal OPC, as illustrated in Fig. 2.

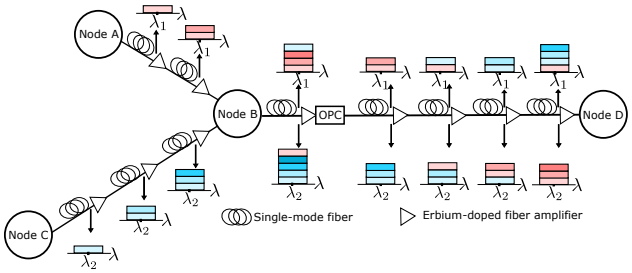

Figure 2: SCI and XCI impairments accumulation and OPC nonlinearity cancellation.

We assumed perfect symmetry around the OPC was achieved, for example using appropriate dispersion management, such that nonlinear distortion arising in paths with equal number of spans before and after the OPC was compensated [12]. This is illustrated in Fig. 2. for the signal propagating from node C to node D. This signal accumulates four spans SCI before the OPC, which are fully compensated by four spans following the OPC (shown in blue). On the other hand, for the signal propagating from node A (shown in red), only six of the seven spans are symmetrically located around an OPC, and so a net SCI corresponding to one span of transmission. For XCI, the mechanism is similar, but only considering the number of spans before and after OPC during which the two signals have co-propagated. In Fig. 2 only the nonlinear XCI arising from the span just before and after the OPC is canceled out for both the blue and the red signals. The SNR of a signal propagating through a path with L links can then be evaluated as:

$$(SNR_i) = \Big(\frac{N_{SpansPath} \cdot P_N}{P_{sig}} + \frac{(N_{SpansPath} - N_{SpansComp}) \cdot P_{SCI}}{P_{sig}} + \frac{\sum_{l=1}^{L} \sum_{j=1}^{J(l)} N_{XCI}(i,j) \cdot P_{XCI}(i,j)}{P_{sig}} \Big)^{-1} \quad (2)$$

where P_{SCI} is the SCI power spectral density, $P_{XCI}(i,j)$ is the XCI power spectral density from the beat between the new signal (i) and each one of the existing signals in the lth link ($j = 1, 2, .., J(l)$), and $N_{XCI}(i,j)$ is the number of spans whose XCI contribution between signals i and j is not compensated.

ISBN: 978-1-61804-355-9

For each new demand all of the following conditions were tested, starting with the highest possible modulation format (Table 1): (i) that spectrum was available in all the links of the path; (ii) that the new signal did not decrease the SNR of the existing signals below their minimum required value to achieve a BER better than 10^{-3}; (iii) that the SNR of the new signal was M times the minimum required SNR (the factor/margin M was included to avoid a signal being routed with only a marginally higher SNR than the minimum required and then blocking all posterior signals due to additional XCI (condition (ii)). If the signal could not be routed because of condition (iii), the process was repeated with a lower-order modulation format with lower a SNR requirements, though with higher spectrum occupancy. If condition (i) was not satisfied, or conditions (ii) or (iii) could not be satisfied with the lowest possible modulation format, the demand was deemed to be blocked. The cumulative blocking probability was calculated as the total number of blocked requests divided by the total number of demands averaged over the total number of simulated runs. At least 500 simulations were performed to obtain the results shown in the next section.

3 Results of the Network simulations

In Fig. 3 we show the obtained blocking probability as a function of the number of demands considering only spectrum assignment (dashed lines) and for the impairment constrained conditions (solid lines). When impairment constrained routing was considered (solid lines) results were plotted for different spectral density values and the modulation formats selected from those listed in Table I.

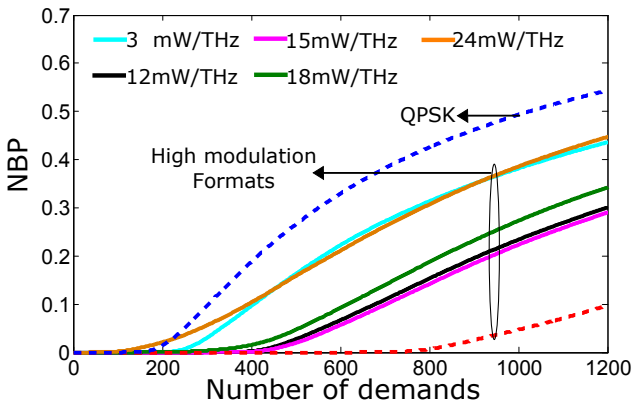

Figure 3: Network blocking probability as a function of the number of demands not including (dashed lines) and including (solid lines) the effects of noise and fiber nonlinearities.

The red dashed lines shown in Fig. 3 shows the maximum potential advantage of using the selected range of high modulation formats in terms of network blocking probability (NBP), resulting from signals with smaller spectrum occupancy. The blue dashed lines shows the NBP when each demand was satisfied by a QPSK signal (constrained only by spectral assignment). In the absence of nonlinearity, the NBP would be reduced to the red curve if the full range of modulation formats (Table I) were used. Obviously, under realistic conditions, that is, considering the physical impairments which affect the quality of the signals transmitted/received, this is only possible as long as the obtained SNR is higher than that required. With no OPCs in the network, a single optimum value of spectral density could be used in all the network, which, as it can be observed in Fig. 3 was around 15mW/THz. For small values (e.g. 3mW/THz) the blocking probability increases due to the increased impact of ASE noise, and for higher values (e.g. 24mW/THz) blocking probability increases due to the fiber nonlinearity. For this network we find that signal impairments reduce the number of supported demands by around 40% compared to spectrum assignment alone.

The underlying objective of using OPCs optical networks is clear: as fiber nonlinearity effects are compensated for, it should be possible to employ higher spectral densities (launch signal powers), increasing the obtained values of SNR and making the transmission of signals with higher modulation formats feasible. By doing so, the obtained NBP curve should be shifted to the right increasing the supported network traffic closer to the maximum defined by spectrum assignment alone (red dashed curve). In order to quantify our results, for each configuration we defined the supported network traffic as the overall traffic at a NBP of 0.05. When ASE and nonlinearities are not included in simulations, around 197Tbits/s and 911Tbits/s are obtained when only DP-QPSK and high modulation formats are employed, corresponding to the blue and red dashed curves in Fig. 3. With impairment constrained routing the maximum supported network traffic was 463Tbits/s or 50% of the maximum possible network capacity. With the inclusion of OPCs, we expect a supported network traffic between these two latter values.

In order to place OPCs in the optical network, we proceeded sequentially placing one OPC after another, in each case selecting the location where largest number of spans may be compensated, assuming one path between each source destination pair in the network. The objective in doing so was to maximise the number of spans with limited number of OPCs without the complexity of an exhaustive search. After

ISBN: 978-1-61804-355-9

placing the first OPC, the interaction between OPCs is also taken into account both increasing and decreasing the net compensation experienced by different signals. OPCs could be placed either at network nodes, or at EDFA sites (we show in Fig. 1 the location of the first four OPCs placed in the optical network using this simple method, all of which were at remote amplifier sites). In Fig. 4 we show the supported network traffic obtained as a function of the maximum value of signal spectral density assumed. Note that since the OPC placement did not allow perfect compensation of all nonlinear effects, XCI dominated the performance and consequently parametric noise amplification [13] was not considered. This assumption is verified by the modest ($\leq$3dB) increase in launch power observed in Fig. 4.

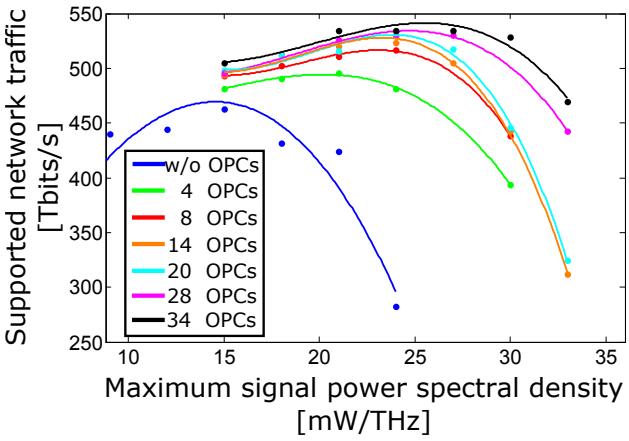

Figure 4: Supported network traffic as a function of the maximum signal power spectral density. Points: results obtained from simulations. Curves: cubic polynomial fitting curve. No OPCs in the optical network: blue curve/points. When OPCs are used, its number ranges from four (green curve/points) to thirty four (black curve/points).

In general, we can observe from Fig. 4 that a higher number of OPCs lead to higher values of supported network traffic, ranging from 495Tbits/s when 4 OPCs are used, to 534Tbits/s when 34 OPCs are used. We can observe also that the highest values of supported network traffic occurs for maximum launch power spectral densities between 21 and 27mW/THz, indicating clearly an increase on the maximum tolerable launch power with respect to the optical network with no OPCs. OPC increases the network capacity by 7 (15)% when 4 (34) devices are placed within the network. Whilst clearly a significant increase in total capacity, the results presented here only enables 54(58)% of the spectrum assignment capacity to be reached. We believe that there are four possible reasons for this. Firstly, rather than exhaustive optimization, both OPC placement and power spectral densities were performed using simple heuristic algorithms. Secondly power spectral densities of existing signals were not re-optimised as additional loads were added. Thirdly, the available signal to noise ratio was not fully exploited due to the discrete set of modulation formats with large differences in required SNR and unused margin M. Finally, in an optical network, it is unlikely to be possible to compensate for all possible XCI without placing an OPC between each and every span.

4 Conclusions

Simulations performed including the effects of SCI and XCI of a sequentially loaded optical network have shown the capability of OPC-based nonlinearity compensation, having achieved substantial improvements for a small number of OPCs. For the example network studied, a network capacity increase of more than 32Tbit/s (7%) was observed using only four OPC devices, rising to 70Tbit/s (15%) for 34 devices. However, the results suggest that further improvements are possible, for example, the launch power policy may be modified in order to prevent signals from being corrupted through links with no nonlinearity compensation. The employment of a more efficient launch power policy to boost the potential improvement as the number of OPCs employed increases is currently a subject of further work.

Acknowledgements: The research was supported by the European Community 7th Framework Program (grant No. 318415 FOX-C) and the EPSRC (grant No. P/L000091/1 PEACE).

References:

[1] S. J. Savory,"Congestion aware routing in nonlinear elastic optical networks," Photon. Technol. Lett., **26**(10), 1057–1060, 2014.

[2] P. Wright, A. Lord, L. Velasco, "The network capacity benefits of Flexgrid," at the Conference on Optical Network design and Modeling, 7–12, 2013.

[3] D. J. Ives, P. Bayvel, S. J. Savory, "Routing, modulation, spectrum and launch power assignment to maximize the traffic throughput of a nonlinear optical mesh network," Photon. Netw. Commun., **29**(3), 244–256, 2015.

[4] R-J. Essiambre, G. Kramer, P. J. Winzer, G. J. Foschini, B. Goebel, "Capacity limits of optical fiber networks," J. Lightw. Technol., **28**(4), 662–701, 2010.

[5] A. D. Ellis, M. E. McCarthy, M. A. Z. Al-Khateeb, S. Sygletos,"Capacity limits of systems employing multiple optical phase conjugators," Opt. Express, **23**(16), 20381–20393, 2015.

[6] I. Sackey et. al., "Kerr nonlinearity mitigation: mid-link spectral inversion versus digital backpropagation in 5×28-GBd PDM 16-QAM signal transmission," J.Lightw. Technol. **33**(9), 1821–1827 (2015).

[7] D. Rafique, J. Zhao, A. D. Ellis,"Digital backpropagation for spectrally efficient WDM 112 Gbit/s PM m-ary QAM transmission," Opt. Express, **19**(6), 5219–5224, 2011.

[8] G. P. Agrawal, *Fiber-optic communications systems* (Wiley, 1997).

[9] P. Poggiolini, "The GN model of non-linear propagation in uncompensated coherent optical systems," J. Lightw. Technol., **30**(24), 3857–3879, 2012.

[10] K. Cho and D. Yoon,"On the general BER expression of one and two-dimensional amplitude modulations," IEEE Trans. Commun., **50**(7), 1074–1030, 2002.

[11] J. M. Simmons, *Optical network design and planning* (Springer, 2008).

[12] D. Rafique and A. D. Ellis, "Various nonlinearity mitigation techniques employing optical and electronic approaches," Photon. Technol. Lett., **23**(23), 1838–1840 (2013).

[13] A. D. Ellis, S. Sygletos, "The Potential for Networks with Capacities Exceeding the Nonlinear Shannon Limit," in Photonic Networks and Devices (PND), Invited Paper, (2015).

ISBN: 978-1-61804-355-9